FEBS Letters 584 (2010) 3107–3110

FEBS Letters

journal homepage: www.FEBSLetters.org

Acid-sensing ion channel (ASIC) 1a undergoes a height transition in response to acidification

Masatoshi Yokokawa [a], Stewart M. Carnally [b], Robert M. Henderson [b], Kunio Takeyasu [c], J. Michael Edwardson [b,*]

[a] Nanometrics Laboratory, Department of Micro Engineering, Graduate School of Engineering, Kyoto University, Yoshida-Honmachi, Sakyo-ku, Kyoto 606-8501, Japan
[b] Department of Pharmacology, University of Cambridge, Tennis Court Road, Cambridge CB2 1PD, United Kingdom
[c] Laboratory of Plasma Membrane and Nuclear Signaling, Graduate School of Biostudies, Kyoto University, Yoshida Konoe-cho, Sakyo-ku, Kyoto 606-8501, Japan

ARTICLE INFO

Article history:
Received 21 April 2010
Revised 20 May 2010
Accepted 24 May 2010
Available online 1 June 2010

Edited by Maurice Montal

Keywords:
Acid-sensing ion channel
Atomic force microscopy
Ion channel structure
Channel activation

ABSTRACT

The acid-sensing ion channel (ASIC) 1a is known to assemble as a homotrimer. Here, we used atomic force microscopy to image ASIC1a, integrated into lipid bilayers, at pH 7.0 and pH 6.0. The triangular appearance of the channel was clearly visible. A height distribution for the channels at pH 7.0 had two peaks, at 2 and 4 nm, likely representing the intracellular and extracellular domains, respectively. At pH 6.0 the 2-nm peak remained, but the higher peak shifted to 6 nm. Hence, the extracellular domain of the channel becomes 'taller' after acidification.

1. Introduction

Acid-sensing ion channels (ASICs) belong to the degenerin/epithelial Na^+ channel family of cation channels (reviewed in [1]). They are activated by extracellular protons and are selectively permeable to Na^+ ions. There are four ASIC genes, which produce six subunit isoforms: ASIC1a, ASIC1b, ASIC2a, ASIC2b, ASIC3, and ASIC4. These subunits assemble to form both homo- and heteromultimers with varying properties, including differential sensitivity to pH [2] and permeability to Ca^{2+} [3]. ASICs are found in all vertebrates, and are responsible for acid-evoked currents in many types of neuron in the peripheral and central nervous systems. They are involved in physiological functions as diverse as nociception, learning and memory, and in pathological conditions such as ischemic stroke. Electrophysiological analysis of the human ASIC1a endogenously expressed in HEK-293 cells [4], revealed that the channel is inactive at pH 7.0 and maximally active at pH 6.0, with half-maximal activation occurring at pH 6.45. Desensitization of the channel is rapid, with a time constant for inactivation of the proton-gated current, measured in whole-cell recordings, of about 1 s.

Each ASIC subunit spans the membrane twice, and the N- and C-termini are intracellular (reviewed in [1]). The recent determination of the crystal structure of chicken ASIC1 at low pH showed that the channel is a trimer [5], and this trimeric structure was confirmed by atomic force microscopy (AFM) imaging of human ASIC1a [6,7]. The availability of the crystal structure has encouraged speculation as to how proton binding to the channel is translated into channel gating [5], although so far there is no direct structural information about this. In the current study, we have taken advantage of the ability of AFM to provide images of proteins in their native environment to investigate the structure of human ASIC1a before and after acidification. We show that acidification causes a significant increase in the height of the channel above the lipid bilayer in which it is integrated.

2. Materials and methods

2.1. Expression, solubilization and purification of ASIC1a

HEK-293 cells, stably transfected with human ASIC1a bearing a C-terminal His_8 tag, were grown in Dulbecco's modified Eagle's medium supplemented with 10% (v/v) newborn calf serum, 100 units/ml penicillin, 100 μg/ml streptomycin, and 100 μg/ml

Abbreviations: ASIC, acid-sensing ion channel; AFM, atomic force microscopy; CHAPS, 3-[(3-cholamidopropyl)dimethylammonio]-1-propanesulfonate; HBS, HEPES-buffered saline

* Corresponding author. Fax: +44 1223 334100.
E-mail address: jme1000@cam.ac.uk (J.M. Edwardson).

0014-5793/$36.00
doi:10.1016/j.febslet.2010.05.050

Zeocin (Invitrogen, Paisley, UK) in an atmosphere of 5% CO_2/air. Protein expression and intracellular localization were checked by immunofluorescence analysis of small-scale cultures. Cells were fixed, permeabilized, and incubated with a rabbit polyclonal antibody against ASIC1a (Alomone, Buckingham, UK). This antibody was raised against residues 469–488 of rat ASIC1; it also recognizes human ASIC1a, as demonstrated previously by both immunofluorescence and immunoblotting [6,7]. Primary antibody was visualized using Cy3-conjugated goat anti-rabbit secondary antibody (Sigma, Poole, UK), and confocal laser scanning microscopy.

Solubilization and purification were performed as described previously [7,8]. Briefly, a crude membrane fraction prepared from the cells was solubilized in 1% (w/v) 3-[(3-cholamidopropyl)dimethylammonio]-1-propanesulfonate (CHAPS), and the solubilized material was incubated with Ni^{2+}-agarose beads (Probond; Invitrogen). The beads were washed extensively with HEPES-buffered saline (HBS) containing 0.5% CHAPS and bound proteins were eluted in the same buffer containing 500 mM imidazole. Samples were analyzed by SDS–polyacrylamide gel electrophoresis. Proteins were detected by silver staining or immunoblotting, using the rabbit polyclonal anti-ASIC1a antibody described above. A typical yield of ASIC1a from 5×162 cm^2 flasks of cells was about 1 μg.

2.2. Integration of ASIC1a into liposomes

1,2-Dioleoyl-*sn*-glycero-3-phosphatidylcholine (DOPC) and brain L-α-phosphatidylserine (PS), obtained from Avanti Polar Lipids (Birmingham, AL) as chloroform stocks, were mixed in the molar ratio of 3:1. The chloroform was evaporated under a stream of nitrogen gas, and the lipids were dissolved in HBS containing 2% CHAPS, to give a total lipid concentration of 2 mg/ml. A 100-μl (200-μg) sample of solubilized lipid was mixed with 1 μg of purified ASIC1a (in a volume of 100 μl), and the resulting mixture was dialysed against a large volume of detergent-free HBS at room temperature for 3 days, with repeated changes of buffer.

2.3. AFM imaging of supported lipid bilayers containing ASIC1a

Proteoliposomes (2 μl) were allowed to adsorb to freshly-cleaved 1 mm^2 mica disks to form supported proteolipid bilayers. After a 15-min incubation, the samples were washed and mounted in the imaging chamber. Imaging was performed under fluid with an NVB500 high-speed atomic force microscope (Olympus, Japan), using tapping mode. The imaging buffer was 100 mM NaCl containing 5 mM MES-NaOH at either pH 7.0 or pH 6.0. Small silicon nitride cantilevers were used (BL-AC7EGS-A2, Olympus, Japan). Each cantilever had a sharp probe that had been deposited using electron beam deposition. The cantilevers had a resonant frequency in water of 600–1,000 kHz and spring constants of 0.1–0.2 Nm^{-1}. Typical free oscillation amplitudes during imaging were approximately 4 nm, and the amplitude set-point was typically approximately 70% of this value.

3. Results

Immunofluorescence analysis of HEK-293 cells stably expressing ASIC1a bearing a His_8 epitope tag at its C-terminus, using an anti-ASIC1a antibody, revealed the presence of ASIC1a channels in the transfected cells (Fig. 1A). The staining pattern indicated that the channels were present both at the plasma membrane and in internal membranes. A crude membrane fraction prepared from the ASIC1a-expressing cells was solubilized in CHAPS detergent (1% w/v), and ASICs were isolated through the binding of the His_8 tag to Ni^{2+}-agarose beads followed by elution with 500 mM imidazole. Both the membrane fraction and the isolated protein were subjected to SDS–PAGE, silver staining, and immunoblotting using the anti-ASIC1a antibody. A silver stain of the isolated fraction (Fig. 1B, left panel) showed a single major band at a molecular mass of 70 kDa, consistent with the expected size of the ASIC1a subunit [9]. The anti-ASIC1a antibody also labeled a single band, again at a molecular mass of 70 kDa (Fig. 1B, right panel). Hence, the isolation procedure produced highly purified ASIC1a, as reported previously [6,7].

Purified ASIC1a was integrated into liposomes (PC/PS; 3:1), and the proteoliposomes were deposited onto mica to produce supported proteolipid bilayers. AFM imaging of these bilayers at pH 7.0 (Fig. 1C) revealed a smooth layer containing numerous small particles, and occasional gaps. A section taken through two gaps (Fig. 1D) revealed a height difference of about 5 nm, consistent with the accepted thickness of a lipid bilayer [10]. Hence, the

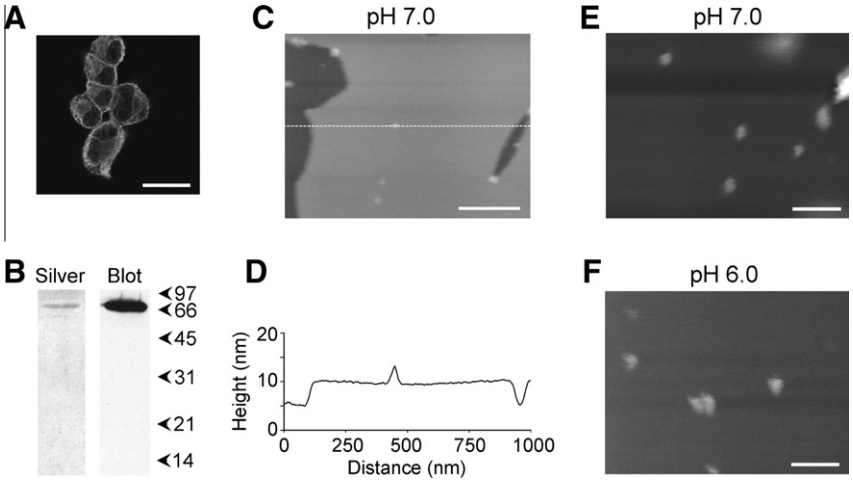

Fig. 1. Isolation of ASIC1a and integration into lipid bilayers. (A) Immunofluorescence detection of ASIC1a in stably transfected HEK-293 cells. Cells were fixed, permeabilized and incubated with rabbit polyclonal anti-ASIC1a antibody, followed by Cy3-conjugated goat anti-rabbit secondary antibody. Cells were imaged by confocal laser scanning microscopy. Scale bar, 20 μm. (B) Isolation of ASIC1a from a membrane fraction of stably transfected cells. Samples were analyzed by SDS–polyacrylamide gel electrophoresis and either silver staining (left-hand panel) or immunoblotting (right-hand panel), using rabbit polyclonal anti-ASIC1a antibody, followed by a horseradish peroxidase-conjugated goat anti-rabbit secondary antibody. Immunoreactive bands were visualized using enhanced chemiluminescence. Arrowheads indicate molecular mass markers (kDa). (C) Low-magnification AFM image of a supported lipid bilayer containing integrated ASICs at pH 7.0. Scale bar, 200 nm. Height range, 20 nm. (D) Section through the bilayer shown in (C), taken at the position indicated by the dotted line. (E) Medium-magnification image of a bilayer at pH 7.0. Scale bar, 100 nm. Height range, 20 nm. (F) Medium-magnification image of a bilayer at pH 6.0. Scale bar, 100 nm. Height range, 20 nm.

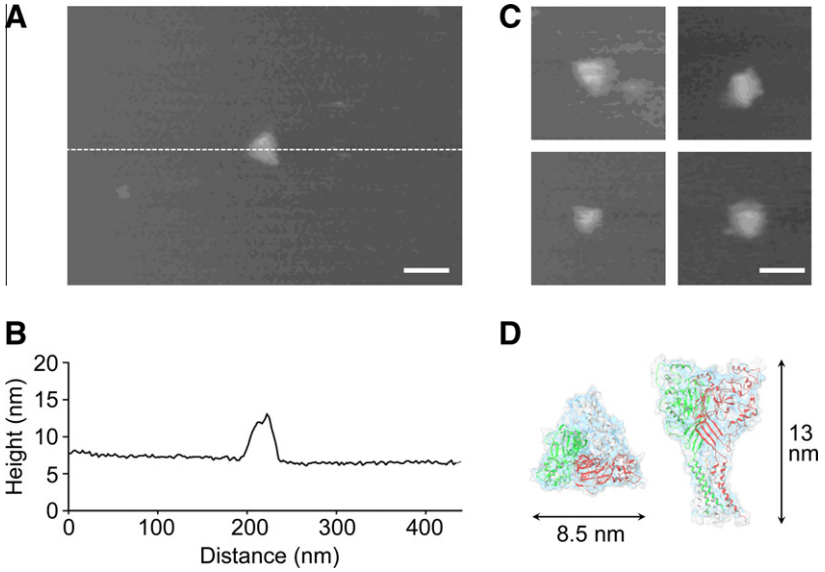

Fig. 2. AFM analysis of the structure of ASIC1a. High-magnification AFM image of a single ASIC1a particle, taken at pH 6.0, showing the triangular appearance of the channel when viewed from the top. (B) Section of the particle, taken at the position indicated by the line in (A). (C) Gallery of images of ASIC1a particles, taken at pH 6.0. (D) Schematic representation of the crystal structure of the ASIC1a trimer (pdb 2QTS) [5]. The top view (left) and the side view (right) of secondary structure ribbon diagrams (red, green and white ribbons, to denote the individual subunits) and van der Waals space (translucent blue) of the ASIC1a trimer are shown, for purposes of comparison with the dimensions shown in (A) and (B). Scale bars, 50 nm.

image likely shows a single bilayer on the mica support. On some occasions, after prolonged incubation of the mica with proteoliposomes, multiple bilayers were seen (data not shown). However, much more commonly, only a single bilayer was present, and only particles in the single bilayers were used for the analysis described below. Note that the section in Fig. 1D also passes through a particle in the bilayer, which protrudes above the bilayer by about 4 nm. Fig. 1E shows a higher-magnification image taken at pH 7.0. A similar overall appearance was seen when imaging was carried out at pH 6.0 (Fig. 1F). We have shown previously in a number of studies (e.g. [11]) that protein-free lipid bilayers are flat and featureless. We conclude, therefore, that the particles in the bilayer are integrated ASICs.

Examination of the structure of the integrated ASICs at high magnification revealed some interesting features. For instance, a top view of some of the proteins showed a clear triangular appearance (see example in Fig. 2A, taken at pH 6.0). A section through the particle (Fig. 2B) showed that its height above the bilayer was about 7 nm. A gallery of similar particles is shown in Fig. 2C. These dimensions are consistent with the crystal structure of the low-pH form of ASIC1a, which also shows a triangular structure when viewed from the extracellular space, and a height above the bilayer of about 8 nm (Fig. 2D). Note that while AFM is able to determine heights to within a fraction of a nanometer, the measurement of widths is much less accurate, because of convolution introduced by the geometry of the scanning tip. For this reason, the measured width of the ASIC particles was significantly greater than the expected value (compare Fig. 2B with Fig. 2D).

We were interested in whether the dimensions of ASIC1a changed in response to changes in pH. To this end, we analysed images of a large number of particles at pH 7.0 (when the channel should be inactive) and at pH 6.0 (which should activate it, and then desensitize it). The results obtained are shown in Fig. 3. At pH 7.0 the frequency distribution of particle heights above the bilayer showed two peaks, at 1.7 ± 0.6 nm (mean ± S.D.) and 4.1 ± 1.5 nm (n = 290; Fig. 3A). At pH 6.0, the distribution again had two peaks, at 2.1 ± 0.7 and 6.3 ± 1.4 nm (n = 189). Our interpretation of these results is illustrated in Fig. 3C and D. We suggest that the two height peaks represent ASICs that have become integrated into the bilayers either extracellular domain down (the low peak) or extracellular domain up (the high peak). The domains protruding beneath the bilayer would be difficult to detect because of the smoothing effect of the bilayer, which is closely apposed to the mica support. The numbers of particles in the two peaks were approximately similar at both pH values, indicating a random insertion of ASIC1a into the bilayer. According to this interpretation, the extracellular domain is significantly higher at low pH than at neutral pH, indicating that a large conformational change occurs during channel activation and desensitization. Because we were unable to measure particle widths accurately, we could not test whether the particles became thinner as well as taller upon acidification, as would be expected.

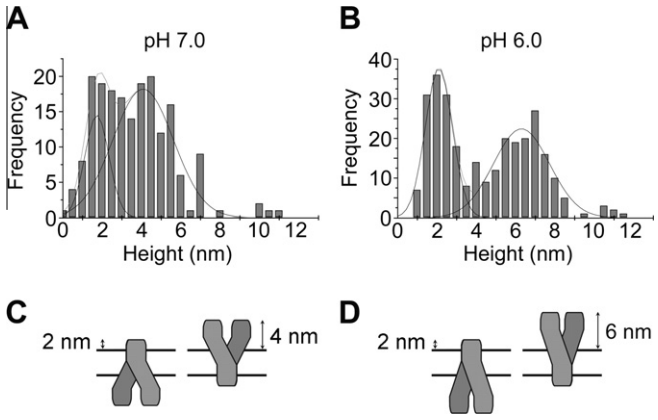

Fig. 3. Effect of acidification on the height of the ASIC1a trimer. (A) Frequency distribution of heights of ASIC1a particles at pH 7.0. The data were collected using seven separate mica samples. The curves indicate the fitted Gaussian functions. (B) Frequency distribution of heights of ASIC1a particles at pH 6.0. The data were collected using four separate mica samples. The curves indicate the fitted Gaussian functions. (C and D) Schematic representations of the suggested ASIC orientations in the bilayer.

4. Discussion

Various techniques have been used to address the structural changes involved in the activation of protein complexes such as neurotransmitter receptors and ion channels. Prominent among these are X-ray crystallography of the proteins in various states, determination of the accessibility of strategic residues to chemical modification, and fluorescence based techniques, such as fluorescence resonance energy transfer. Thanks to these studies, rapid progress is being made towards understanding the relationship between structure and function of protein complexes such as the Cys-loop receptors (reviewed in [12]), the glutamate receptors (reviewed in [13]), the P2X receptors (reviewed in [14]) and the voltage-activated potassium channels (reviewed in [15]). It has proven difficult, however, to directly visualize structural changes at the single molecule level. The ability of AFM to image individual proteins under near-physiological conditions, has placed it at the forefront of this approach.

In the current study, we have shown that ASIC1a undergoes a profound structural change in response to acidification, with its height above the bilayer increasing from 4 to 6 nm when pH falls from 7.0 to 6.0. Given the rapid desensitization of ASIC1a [4], the low-pH form almost certainly represents the desensitized form. To understand the structural arrangements occurring as the channel passes from the inactive state through the active state and into the desensitized state it will be necessary to image the channel using fast-scan AFM during the process of acidification, a feat that we have not so far achieved.

Direct observation of structural changes involved in receptor activation by fast-scan AFM was in fact reported recently for the P2X4 receptor, which, like ASIC1a, assembles as a homotrimer [16]. The structure of the P2X4 receptor shows several important differences from the structure of ASIC1a that we report here. For instance, the inactive P2X4 receptor was much lower (about 2 nm above the bilayer), although as for ASIC1a, there did appear to be an increase in the height of P2X4 after activation by ATP. Further, activation by ATP triggered the spreading out of the receptor so that the three individual subunits could be clearly discerned, which was not the case for ASIC1a. The results of these two studies indicate that a basic similarity in assembly state might mask considerable differences in structural response to activation.

We suggest that further application of AFM imaging might shed significant new light on the structural rearrangements occurring during the activation and desensitization of receptors and ion channels.

Acknowledgements

This work was supported by a grant from the BBSRC (BB/D015545/1) to RMH and JME, a BBSRC Japan Partnering Award to RMH and JME, a JSPS Japan-UK Bilateral Joint Project Award to KT, and a JSPS Grant-in-Aid for Basic Research to KT.

References

[1] Wemmie, J.A., Price, M.A. and Welsh, M.J. (2006) Acid-sensing ion channels: advances, questions and therapeutic opportunities. Trends Neurosci. 29, 578–586.
[2] Benson, C.J., Xie, J., Wemmie, J.A., Price, M.P., Henss, J.M., Welsh, M.J. and Snyder, P.M. (2002) Heteromultimers of DEG/ENaC subunits form H^+-gated channels in mouse sensory neurons. Proc. Natl. Acad. Sci. USA 99, 2338–2343.
[3] Yermolaieva, O., Leonard, A.S., Schnizler, M.K., Abboud, F.M. and Welsh, M.J. (2004) Extracellular acidosis increases neuronal cell calcium by activating acid-sensing ion channel 1a. Proc. Natl. Acad. Sci. USA 101, 6752–6757.
[4] Gunthorpe, M.J., Smith, G.D., Davis, J.B. and Randall, A.D. (2001) Characterisation of a human acid-sensing ion channel (hASIC1a) endogenously expressed in HEK293 cells. Pflügers Arch. Eur. J. Physiol. 442, 668–674.
[5] Jasti, J., Furukawa, H. and Gouaux, E. (2007) Structure of acid-sensing ion channel 1 at 1.9 Å resolution and low pH. Nature 449, 316–323.
[6] Carnally, S.M., Dev, H.S., Stewart, A.P., Barrera, N.P., van Bemmelen, M.X., Schild, L., Henderson, R.M. and Edwardson, J.M. (2008) Direct visualization of the trimeric structure of the ASIC1a channel, using AFM imaging. Biochem. Biophys. Res. Commun. 372, 752–755.
[7] Carnally, S.M., Johannessen, M., Henderson, R.M., Jackson, M.B. and Edwardson, J.M. (2010) Demonstration of a direct interaction between σ-1 receptors and acid-sensing ion channels. Biophys. J. 98, 182–1191.
[8] Barrera, N.P., Ormond, S.J., Henderson, R.M., Murrell-Lagnado, R.D. and Edwardson, J.M. (2005) AFM imaging demonstrates that P2X2 receptors are trimers but that P2X6 receptor subunits do not oligomerize. J. Biol. Chem. 280, 10759–10765.
[9] Meltzer, R.H., Kapoor, N., Qadri, Y.J., Anderson, S.J., Fuller, C.M. and Benos, D.J. (2007) Heteromeric assembly of acid-sensitive ion channel and epithelial sodium channel subunits. J. Biol. Chem. 282, 25548–25559.
[10] Sprong, H., van der Sluijs, P. and van Meer, G. (2001) How proteins move lipids and lipids move proteins. Nat. Rev. Mol. Cell. Biol. 2, 504–513.
[11] Lawrence, J.C., Saslowsky, D.E., Edwardson, J.M. and Henderson, R.M. (2003) Real-time analysis of the effects of cholesterol on lipid raft behavior using atomic force microscopy. Biophys. J. 84, 1827–1832.
[12] Karlin, A. (2002) Emerging structure of the nicotinic acetylcholine receptors. Nat. Rev. Neurosci. 3, 102–114.
[13] Mayer, M.L. (2006) Glutamate receptors at atomic resolution. Nature 440, 456–462.
[14] Khakh, B.S. and North, R.A. (2006) P2X receptors as cell-surface ATP sensors in health and disease. Nature 442, 527–532.
[15] MacKinnon, R. (2003) Potassium channels. FEBS Lett. 555, 62–65.
[16] Shinozaki, Y., Sumitomo, K., Tsuda, M., Koizumi, S., Inoue, K. and Torimitsu, K. (2009) Direct observation of ATP-induced conformational changes in single P2X4 receptors. PLoS Biol. 7, e1000103.